Electronic Supplementary Material (ESI) for RSC Advances.

Tailoring Nanoscale Polarization Patterns in Ferroelectric Tunnel Junctions by Octahedral Tilts in Electrodes

Hongfang Li*, Weijin Chen and Yue Zheng

School of Materials Science and Engineering, Chongqing Jiaotong University, Chongqing, 400074, China.

*E-mail: 990201600012@cqjtu.edu.cn

Supplementary Information

8 possible $SrRuO_3$/($BaTiO_3$/$CaTiO_3$) interfaces for the simulated FTJs are shown in Fig. S1, where (1) to (4) are perovskite-type interfaces and (7), (8) are rocksalt-type interfaces. Interface cohesive energy E_{co} is defined as the energy gained by combine the barrier with electrodes to form a FTJ:

$$E_{co} = (E_{SrRuO_3} + E_{BaTiO_3/CaTiO_3} - E_{SrRuO_3/(BaTiO_3/CaTiO_3)})/2S\,, \qquad (1)$$

where E_{SrRuO_3} is the total energy of $SrRuO_3$ electrodes, $E_{BaTiO_3/CaTiO_3}$ is the total energy of the $BaTiO_3$/$CaTiO_3$ barrier, $E_{SrRuO_3/(BaTiO_3/CaTiO_3)}$ is the total energy of the FTJ, and S is the area of the interface. Calculated E_{co} and averaged interface distances for 8 types of interfaces are shown in Tab. SI, it is clear that interface (3) and (4) have highest cohesive energies with shortest averaged interface distances. Therefore only two types of FTJs are considered in the following: FTJ #1 has type (3) of interfaces and FTJ #2 has type (4) of interfaces, as shown on the right of Fig. S1. Each FTJ consists of 7 monolayers of bottom electrode, 7 monolayers of ferroelectric barrier and 7 monolayers of top electrode, and symmetric interfaces are applied to both of them.

An interesting fact is that from Tab. SI, the cohesive energy generally decreases with the increase of averaged interface distance, but although interface (4) has a larger averaged distance than interface (3), they have very close cohesive energy. Further investigation of interface atom configurations is performed to explain this result. From the atom configurations near bottom interface in FTJ #1 and #2, it can be seen that octahedral tilts in barrier are significant suppressed in FTJ #1 while it can be retained in FTJ #2. Therefore, the interfacial TiO_2 layer is highly deformed along z-

direction in FTJ #2 due to octahedral tilts, which drastically increased the averaged interface distance. However, the minimum interface distance in FTJ #2 (i. e. The distance between the nearest two atoms on different sides of the interface) is 1.68Å, which is significantly smaller than 1.89Å of FTJ #1. This indicates that interface (4) is actually more closely packed than interface (3), thus interface (4) is more stable and has a higher cohesive energy.

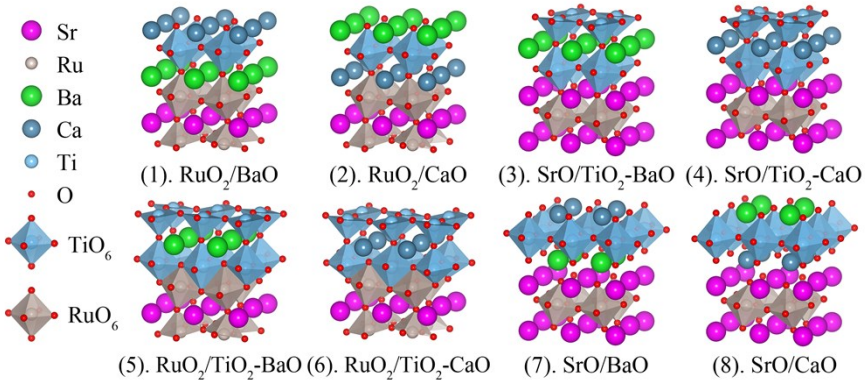

Figure. S1. Schematic illustrations of 8 possible heterointerfaces between $SrRuO_3$ and 1:1 $BaTiO_3$-$CaTiO_3$ superlattice: (1) RuO_2/BaO interface, (2) RuO_2/CaO interface, (3) SrO/TiO_2-BaO interface, (4) SrO/TiO_2-CaO interface, (5) RuO_2/TiO_2-BaO interface, (6) RuO_2/TiO_2-CaO interface, (7) SrO/BaO interface, and (8) SrO/CaO interface. From (1) to (4) are perovskite interfaces, and (7), (8) are rocksalt interfaces.

Interface	E_{co}(eV/Å^2)	$\bar{u}$(Å)
(1)RuO_2/BaO	0.167	1.997
(2)RuO_2/CaO	0.176	1.989
(3)SrO/TiO_2-BaO	0.196	1.922
(4)SrO/TiO_2-CaO	0.198	1.941
(5)RuO_2/TiO_2-BaO	0.160	2.145
(6)RuO_2/TiO_2-CaO	0.156	2.148
(7)SrO/BaO	0.078	2.444
(8)SrO/CaO	0.117	2.426

TABLE. SI Calculated cohesive energies and averaged interface distances for different interfaces between $SrRuO_3$ and 1:1 $BaTiO_3$/$CaTiO_3$ superlattice